

Anhydrous Protonic Conductivity of a Self-Assembled Acid–Base Composite Material

Masanori Yamada and Itaru Honma*

Energy Electronic Institute, National Institute of Advanced Industrial Science and Technology (AIST),
Umezono 1-1-1, Tsukuba, Ibaraki 305-8568, Japan

Received: June 18, 2003; In Final Form: October 15, 2003

Recently, anhydrous proton-conducting membranes have attracted remarkable interest for application to the polymer electrolyte membrane fuel cell (PEMFC) operated at intermediate temperature (100–200 °C). In this paper, we prepared the self-assembled acid–base composite material with the highly ordered molecular array through the hybridization of acidic surfactant monododecyl phosphate (MDP) and basic surfactant 2-undecylimidazole (UI) molecules. This UI–MDP composite material has been found to form highly ordered lamellar structures with a d spacing of approximately 40 Å and to construct two-dimensional proton-conducting pathways within the close-packed surfactant headgroups. As a result, UI–MDP lamellar composite materials showed a high proton conductivity of $1 \times 10^{-3} \text{ S cm}^{-1}$ at 150 °C under the anhydrous condition. Additionally, the activation energy, 0.30–0.45 eV, of proton conduction was almost the same as for other materials reported as anhydrous single-proton conductors. These anhydrous proton-conducting materials without the existence of water molecules are quite different for ion-exchange membranes such as Nafion and may have advantages as an electrolyte membrane for PEMFC.

Introduction

The operation of polymer electrolyte membrane fuel cells (PEMFC) at intermediate temperature (100–200 °C) has been considered to provide many advantages such as improved carbon monoxide tolerance of the Pt electrode, reduction of the amount of Pt electrode materials, higher energy efficiency, heat managements, and cogenerations.^{1–6} However, customary electrolyte membranes, such as humidified Nafion, are unstable at higher temperature, and proton conductivity decreases by the evaporation of water from the membrane and degradations of the molecular structure by irreversible reactions.^{7,8} Therefore, an electrolyte membrane with high proton conductivity at intermediate temperatures under anhydrous or low-humidity conditions has attracted much interest recently for problem solving in the current technologies.^{1–6} From this viewpoint on acid–base complex electrolyte membranes, attention has been focused.^{9–14} In particular, composite materials of strong acids, such as phosphoric acid or sulfuric acid, or basic heterocycle molecules, such as imidazole and benzimidazole, have been found to show a high proton conductivity under anhydrous (low-humidity) and intermediate-temperature conditions.^{2,6,15–21}

The proton transport of an acid–base composite material under anhydrous or low-humidity conditions is supposed to occur by a Grotthuss mechanism,²² in which only protons are mobile from site to site without the presence of diffusible water molecules, such as H_3O^+ or H_5O_2^+ . Therefore, the molecular structure of the acid–base composite material is crucial for the rate of proton transport.^{23–25} Namely, an existence of a proton-conductive pathway in the membrane is one of the most important factors for the high conductivity. However, the simple mixing of acidic and basic molecules generally forms a random proton-conductive pathway and, as a result, does not provide the maximum conductivity that can be reached for that acid–base

complex. If the proton-conductive pathway is controlled by a suitable molecular assembly between acidic and basic moieties, the highest protonic conductivity will be obtained.

In this paper, we prepared a self-assembled acid–base complex consisting of acidic surfactant monododecyl phosphate (MDP) and basic surfactant 2-undecylimidazole (UI) molecules with long hydrophobic chain. This UI–MDP composite material possesses lamellar structures with two-dimensional proton-conductive pathways of acidic and basic headgroups and, as a result, exhibits a high proton conductivity of $1 \times 10^{-3} \text{ S cm}^{-1}$ at 150 °C under the anhydrous condition.

Experimental Section

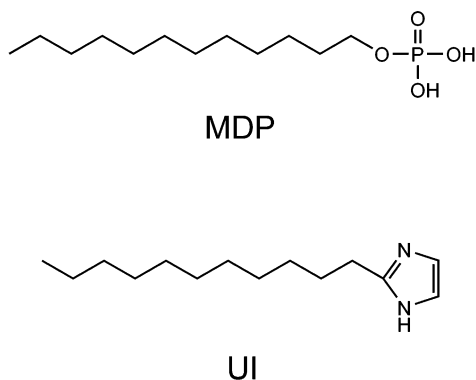
Materials. MDP, UI, and imidazole (Im) were obtained from Alfa Aesar, a Johnson Matthey Co., MA; Wako Pure Chemical Industries, Ltd., Osaka, Japan; and Tokyo Kasei Kogyo Co., Ltd., Tokyo, Japan, respectively. Molecular structures are shown in Chart 1. Glass filters (thickness, 0.2 mm) were purchased from Advantec Toyo Kaisha, Ltd., Tokyo, Japan. Solvents were used at an analytical grade in all the experiments described.

Preparation of UI–MDP Composite Materials. Samples of proton-conductive measurements were prepared by supporting the glass filter as following: UI (50 or 100 mg/mL) and MDP (50 mg/mL) were dissolved in ethanol. The UI (40 or 20 μL) and MDP solutions were simultaneously cast onto a glass filter ($7 \times 7 \times 0.2 \text{ mm}^3$) and dried for 2 h at room temperature. This process was repeated five times. The total amount of UI in the UI–MDP composite materials was 10 mg. The Im–MDP composite material was also prepared by the same method.

Characterizations of Composite Materials. The molecular orientation of the UI–MDP composite material was measured by the polarized light microscopy. The UI–MDP composite ethanol solution was cast onto the slide glass, and the solvent was evaporated from the sample. Then, the materials were observed by optical microscopy (BX51, Olympus Optical Co., Ltd., Tokyo, Japan) with two polarized light lenses. The

* Author to whom correspondence may be addressed. Tel: +81 29 8615648, Fax: +81 29 8615829. E-mail: i.homma@aist.go.jp.

CHART 1. Molecular Structures of MDP and UI



molecular structure of the UI-MDP composite material was analyzed by X-ray diffraction (XRD) (MO3XHF22, MAC Science Co., Ltd., Yokohama, Japan) with Cu K α radiation ($\lambda = 1.54 \text{ \AA}$). The composite structures were also characterized by IR absorption measurements (FTS-60, Bio-Rad Laboratories, Inc., PA) with the attenuated total reflection (ATR) prism (Golden Gate Diamond ATR System, Specac Ltd., GA). The IR spectrum was measured with a resolution of 4 cm^{-1} .

Conductivity Measurements. Proton conductivity of the UI-MDP composite materials was measured by the ac impedance method in a frequency range from 1 Hz to 1 MHz using an impedance analyzer SI-1260 (Solartron Co., Hampshire, UK) in a stainless vessel from room temperature to 160°C . The glass filter supported the UI-MDP composite materials ($7 \times 7 \times 0.2 \text{ mm}^3$) sandwiched between two gold-coated electrodes (diameter, 5 mm). The direction of conductive measurement is perpendicular to the filter. All measurements in this work were carried out under dry nitrogen flow. So, the measured impedance indicates anhydrous (water-free) proton conductivity of the acid-base composite electrolyte membranes.^{15,16}

Results and Discussions

Basic surfactant UI and acidic surfactant MDP were dissolved in ethanol. The UI and MDP solutions were simultaneously cast onto a glass filter or a glass plate and dried at room temperature. The UI-MDP composite material was also prepared by the same method. Microscopic images of the UI-MDP composite material on a glass plate are shown in Figure 1, where parts a and b indicate the nonpolarized and polarized light microscopic images, respectively. The image of the UI-MDP composite material can be observed under the cross-nicol condition. Additionally, these images under the cross-nicol condition were obtained at all of the parts. These results suggest that the UI-MDP composite materials have ordered structure with the molecular orientation at the wide area of material.

Next, we performed the XRD measurements on the UI-MDP composite materials. Figure 2 shows the XRD pattern of the UI-MDP composite material, where parts a and b indicate the XRD patterns at low- and high-angle regions, respectively. Fundamental (peak 1 in Figure 2a) and associated higher-order (peaks 2–9 in parts a and b of Figure 2) diffraction peaks indicate that highly ordered lamellar structures were formed in the UI-MDP composite material (Table 1). These diffraction peaks of lamellar structures are observed until the ninth order, indicating that the two-dimensional structure is highly uniform. The d spacing of the (001) diffraction peak was calculated to be 39.9 \AA according to the Bragg's equation. According to the Corey–Pauling–Koltun model, the molecular lengths of UI and

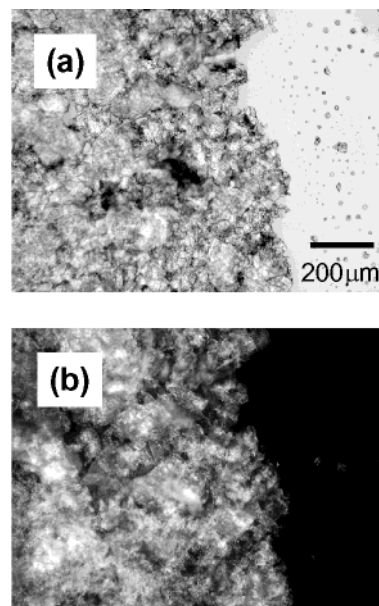


Figure 1. Microscopic images of UI-MDP composite materials. (a) and (b) show the nonpolarized and polarized light microscopic images, respectively. A scale bar is $200 \mu\text{m}$.

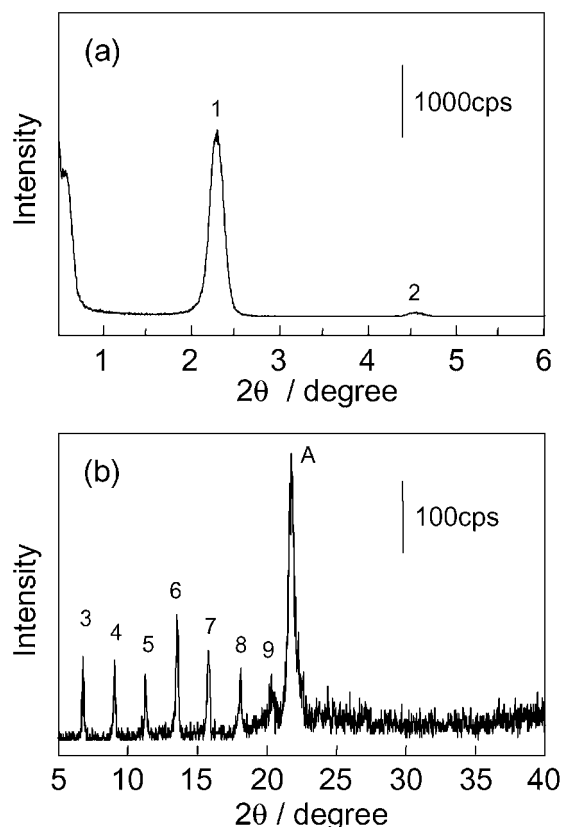


Figure 2. XRD patterns of the UI-MDP composite materials. (a) and (b) show the XRD patterns at low- and high-angle regions, respectively.

MDP were approximately 19.5 and 20 \AA , respectively. So, the d spacing of the lamellar structure is almost equivalent to the summation of the length of acidic or basic surfactants. The result suggests that the UI-MDP composite material takes a tail-tail bilayer membrane conformation. In contrast, the distance between the alkyl chains of the surfactants was calculated to be 4.09 \AA (shown in Figure 2b, peak A, and Table 1) and is the same as the distance between the imidazole molecules with the hydrogen bonding.

TABLE 1: Measured and Calculated d Spacing of the UI-MDP Composite Material

entry	2θ (deg)	d spacing (\AA)	
		XRD	calculation ^a
1	2.21	39.9	39.9
2	4.44	19.9	19.9
3	6.74	13.1	13.3
4	8.94	9.88	9.97
5	11.2	7.88	7.98
6	13.5	6.56	6.65
7	15.8	5.61	5.70
8	18.0	4.93	4.98
9	20.2	4.39	4.43
A	21.7	4.09	

^a These distances of the lamellar structure were calculated from measured d spacing of 39.9 \AA .

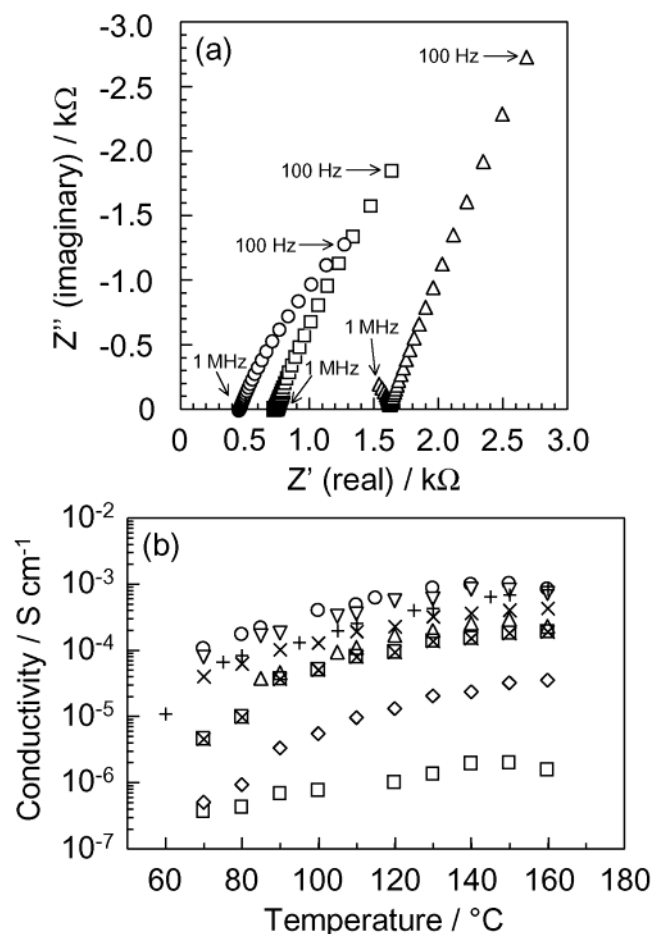


Figure 3. (a) Typical impedance response (Cole–Cole plots) of UI–MDP composite materials at 80 (Δ), 100 (\square), and 120 $^{\circ}\text{C}$ (\circ). (b) Proton conductivities of the UI–MDP composite materials with different MDP doping ratios under anhydrous condition. Measurements were performed under dry nitrogen condition. Doping ratios of MDP are pure UI (\square), 10 wt % MDP composite (Δ), 12.5 wt % MDP composite (\circ), 15 wt % MDP composite (∇), 17.5 wt % MDP composite ($+$), 20 wt % MDP composite (\times), 50 wt % MDP composite (\times in a box), and 100 wt % MDP composite materials (\diamond).

The proton-conductivity measurements of the UI–MDP composite materials were performed by the ac impedance method over the frequency range from 1 Hz to 1 MHz under dry nitrogen flow. Figure 3a showed the typical impedance response (Cole–Cole plots) of the UI–MDP composite materials at 80 (Δ), 100 (\square), and 120 $^{\circ}\text{C}$ (\circ). Typical Cole–Cole plots of composite materials showed a feature similar to that of a highly proton-conducting membrane, such as Nafion, organic/

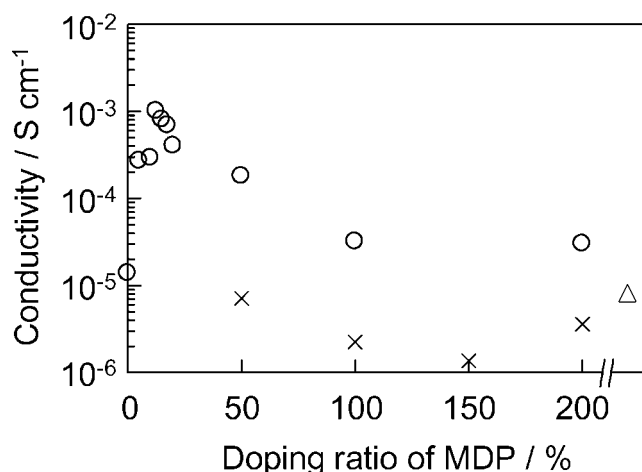


Figure 4. Change of the proton conductivities under anhydrous condition of UI–MDP composite materials (\circ), pure MDP material (Δ), and Im–MDP composite materials (\times). Proton conductive measurements were demonstrated under dry nitrogen condition.

inorganic hybrid membrane mixed with heteropolyacids,^{26–28} MDP/benzimidazole,¹⁵ and poly(vinylphosphonic acid)/heterocycle molecules¹⁶ composite materials. The resistances of the composite material were obtained from the extrapolation to the real axis. Conductivities of the UI–MDP composite materials with different MDP doping ratios of pure UI (\square), 10 wt % MDP composite (Δ), 12.5 wt % MDP composite (\circ), 15 wt % MDP composite (∇), 17.5 wt % MDP composite ($+$), 20 wt % MDP composite (\times), 50 wt % MDP composite (\times in a box), and 100 wt % MDP composite materials (\diamond) in temperatures range from 60 to 160 $^{\circ}\text{C}$ are shown in Figure 3b. The conductivity of pure UI material without MDP doping slightly increases with the temperature and reaches a maximum conductivity of approximately $1 \times 10^{-6} \text{ S cm}^{-1}$ at 150 $^{\circ}\text{C}$. In contrast, proton conductivities of the UI–MDP composite material immediately increase by the addition of MDP molecules. UI–12.5 wt % MDP composite material (mole ratio UI–MDP = 9.6:1) showed the highest conductivity of $1 \times 10^{-3} \text{ S cm}^{-1}$ at 150 $^{\circ}\text{C}$ under anhydrous condition. However, the conductivity becomes smaller when more than 20 wt % of MDP is added. On the other hand, thermal stability of the UI–MDP composite material was analyzed by thermogravimetric and differential thermal analyses. As a result, the composite materials were stable until approximately 170 $^{\circ}\text{C}$. The melting point of the UI–MDP composite material is above 180 $^{\circ}\text{C}$ (data not shown). In fact, the sudden increase in proton conductivity based on the melting or glass transition of the sample was not obtained (see Figure 3b).

Proton conductivities at 150 $^{\circ}\text{C}$ under anhydrous conditions of UI–MDP composite materials (\circ), pure MDP material (Δ), and Im–MDP composite materials (\times), are shown in Figure 4. The anhydrous conductivity of the UI–MDP composite material increased with the doping ratio of MDP and reached the maximum value of $1 \times 10^{-3} \text{ S cm}^{-1}$ at UI–12.5 wt % MDP composite material. This value was 2 orders of magnitude higher than that of pure UI or MDP materials. In contrast, the Im–MDP composite material showed extremely low proton conductivity at 150 $^{\circ}\text{C}$ under anhydrous conditions (shown in Figure 4). In particular, the composite materials with the MDP doping ratio smaller than 50 wt % could not give measurable proton conductivity. These results suggested that high proton conductivity of the UI–MDP composite material was due not only to the concentration of imidazole or phosphonic groups but also to the molecular structure, such as a high-ordered lamellar

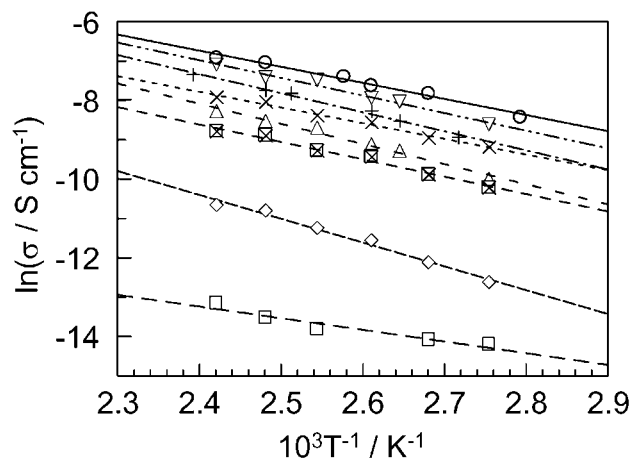


Figure 5. Arrhenius plots of UI-MDP composite materials. Solid lines are results of the least-squares fitting. Activation energies (E_a) of the proton transfer under anhydrous condition were estimated from the slope. Doping ratios of MDP are pure UI (\square), 10 wt % MDP composite (Δ), 12.5 wt % MDP composite (\circ), 15 wt % MDP composite (∇), 17.5 wt % MDP composite ($+$), 20 wt % MDP composite (\times), 50 wt % MDP composite (\times in a box), and 100 wt % MDP composite materials (\diamond).

structure. In fact, the XRD pattern of the Im-MDP composite material did not show the lamellar structure. The self-assembled acid-base pair in the two-dimensional space of the lamellar stacking might offer efficient proton-transfer processes with minimum jumping distances between the molecules.

Finally, we determined the activation energy of proton conduction for UI-MDP composite material. Figure 5 shows the Arrhenius plot of proton conductivity of the UI-MDP composite material. Solid lines in Figure 5 are the results of the least-squares fitting. The activation energies (E_a) estimated

from the slope are 0.30–0.45 eV. The E_a of UI-12.5 wt % MDP composite material is 0.35 eV. This value is almost the same as that for other materials reported as anhydrous single proton conductors, such as the poly(vinylphosphonic acid)/heterocycle composite material.¹⁶ These results supported the fact that the proton-transporting mechanism in the UI-MDP composite material with lamellar structure is not a vehicular mechanism but a proton hopping mechanism of a Grotthuss type. On the other hand, the proton conductivity at low- ($<80^\circ\text{C}$) and high-temperature regions ($>150^\circ\text{C}$) could not fit by the least-squares method. This indicates that the conducting mechanisms of proton are different in the respective regions.

Previously, we reported the proton-conducting membrane of the acid-base composite material with the heterocycle molecule under anhydrous conditions.^{15,16} In this case, a Grotthuss-type diffusion mechanism has been proposed, in which the transport of the proton in basic heterocycle molecules can occur from protonated molecules to nonprotonated neighbor molecules.^{23–25} Namely, their protonated and nonprotonated nitrogen atoms in heterocycle may act as donors and acceptors in proton-transfer reactions.^{23–25} In contrast, acidic molecules, such as phosphoric acid or sulfuric acid, are also described as proton donors and acceptors with the formation of protonic defects (e.g., H_2PO_4^- or HSO_4^-) and are considered to have intermolecular proton-transfer reactions.²⁹ Therefore, the distance between the acidic and basic molecules is important for the formation of an effective proton-conducting pathway in an acid-base composite material. Figure 6 shows the structural model and proton-conducting mechanism of UI-MDP composite material in the self-assembled lamellar structure. The UI and MDP molecules are assembled to form a bilayer lamellar structure with the d spacing of 39.9 Å. The distance between alkyl chains is approximately 4 Å. Namely, the headgroups of the surfactant,

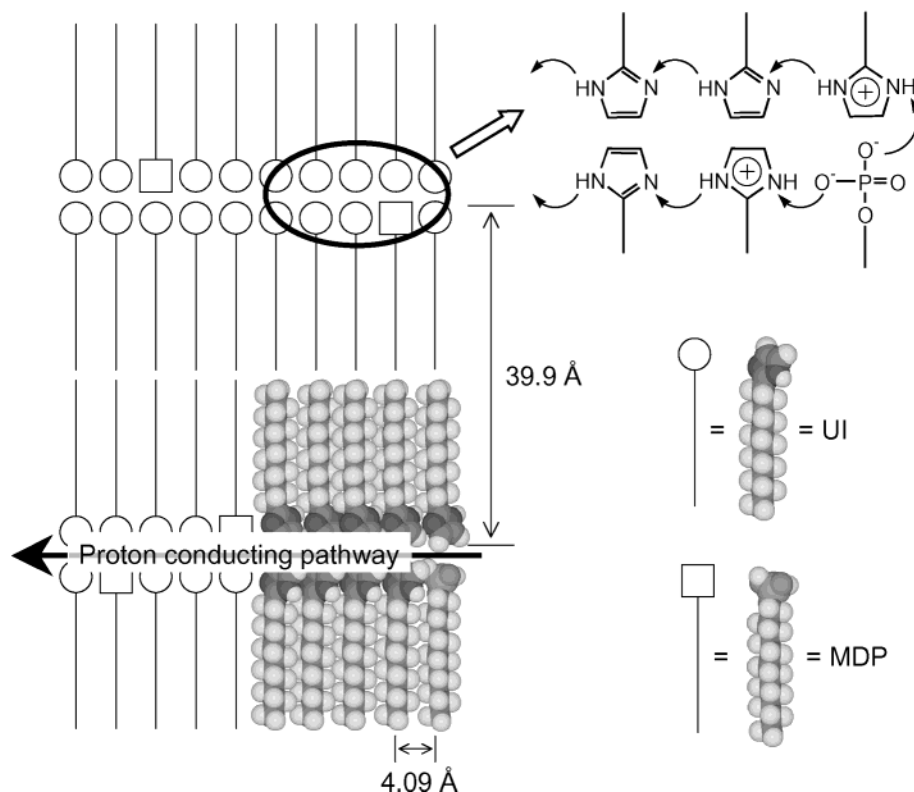


Figure 6. Structural model of UI-MDP composite materials. The UI and MDP molecules construct the highly ordered lamellar structure with the proton-conducting pathway. UI and MDP molecules indicate the space-filling and line-drawings models. The insert shows the proton-conducting mechanism in the two-dimensional proton-conducting pathway.

such as the imidazole or phosphonic acid groups, have assembled in the two-dimensional space with hydrophobic interactions of alkyl chains for close-packed array events. Proton conduction of the UI–12.5 wt % MDP (mole ratio UI–MDP = 9.6:1) composite material must primarily occur as an array of UI molecules because the distance between the MDP molecules is too large. The proton-conduction mechanism is supposed to be as follows (shown in the Figure 6 insert): the imidazole groups were protonated by the proton transfer from neighboring MDP molecules. These acid–base ionic complexes of imidazole and phosphonic acid groups can be confirmed by the IR measurements. The transport of the proton in close-packed heterocycle molecules can occur from protonated molecules to nonprotonated neighboring molecules. Therefore, the head–head distance and the highly ordered assembly of the heterocycle molecules of lamellar structure might play an important role to afford the proton-conducting pathway. As a result, the UI–MDP composite material indicates the high proton conductivity of $1 \times 10^{-3} \text{ S cm}^{-1}$ at 150 °C under the anhydrous condition. These anhydrous proton-conducting materials without the existence of water molecules are extremely novel and practically important as advanced electrolyte membranes for PEMFC operated above the boiling point of water (100 °C).

Conclusions

We have investigated the anhydrous proton-conducting membrane through the composite of acidic surfactant MDP and basic surfactant UI. This UI–MDP composite material is formed by a highly ordered lamellar structure made of a two-dimensional array of acidic and basic headgroups forming the effective proton-conducting pathway. As a result, the composite material showed the high proton conductivity of $1 \times 10^{-3} \text{ S cm}^{-1}$ at 150 °C under the anhydrous condition, i.e., without the presence of water molecules in the electrolyte membrane. The acid–base composite material may have potential application not only for the PEMFC operated at intermediate temperatures under anhydrous (water-free) or extremely low humidity conditions but also novel electrochemical devices including electrochromic displays, chemical sensors, and others, where water activity is not required.

Acknowledgment. This work was supported by the R&D program of PEFC by New Energy and Industrial Technology Development Organization, Japan (NEDO).

References and Notes

- (1) Kerres, J. A. *J. Membr. Sci.* **2001**, *185*, 3.
- (2) Rikukawa, M.; Sanui, K. *Prog. Polym. Sci.* **2000**, *25*, 1463.
- (3) Kreuer, K. D. *J. Membr. Sci.* **2001**, *185*, 29.
- (4) Alberti, G.; Casciola, M. *Solid State Ionics* **2001**, *145*, 3.
- (5) Kreuer, K. D. *ChemPhysChem* **2002**, *3*, 771.
- (6) Kruer, K. D. *Solid State Ionics: Science & Technology*; Chowdari, B. V. R. et al. Eds.; World Scientific Publishing: Singapore, 1998.
- (7) Sone, Y.; Ekdunge, P.; Simonsson, D. *J. Electrochem. Soc.* **1996**, *143*, 1254.
- (8) Sumner, J. J.; Creager, S. E.; Ma, J. J.; Desmarteau, D. D. *J. Electrochem. Soc.* **1998**, *145*, 107.
- (9) Kawahara, M.; Morita, J.; Rikukawa, M.; Sanui, K.; Ogata, N. *Electrochim. Acta* **2000**, *45*, 1395.
- (10) Bouchet, R.; Siebert, E. *Solid State Ionics* **1999**, *118*, 287.
- (11) Noda, A.; Susan, M. A. B. H.; Kudo, K.; Mitsushima, S.; Hayamizu, K.; Watanabe, M. *J. Phys. Chem. B* **2003**, *107*, 4024.
- (12) Susan, M. A. B. H.; Noda, A.; Mitsushima, S.; Watanabe, M. *Chem. Commun.* **2003**, 938.
- (13) Sun, J.; Jordan, L. R.; Forsyth, M.; MacFarlane, D. R. *Electrochim. Acta* **2001**, *46*, 1703.
- (14) Tsuruhara, K.; Rikukawa, M.; Sanui, K.; Ogata, N.; Nagasaki, Y.; Kato, M. *Electrochim. Acta* **2000**, *45*, 1391.
- (15) Yamada, M.; Honma, I. *Electrochim. Acta* **2003**, *48*, 2411.
- (16) Yamada, M.; Honma, I. Submitted.
- (17) Pu, H.; Meyer, W. H.; Wegner, G. *Macromol. Chem. Phys.* **2001**, *202*, 1478.
- (18) Schechter, A.; Savinell, R. F. *Solid State Ionics* **2002**, *147*, 181.
- (19) Bozkurt, A.; Meyer, W. H. *Solid State Ionics* **2001**, *138*, 259.
- (20) Schuster, M.; Meyer, W. H.; Wegner, G.; Herz, H. G.; Ise, M.; Schuster, M.; Kreuer, K. D.; Maier, J. *Solid State Ionics* **2001**, *145*, 85.
- (21) Herz, H. G.; Kreuer, K. D.; Maier, J.; Scharfenberger, G.; Schuster, M. F. H.; Meyer, W. H. *Electrochim. Acta* **2003**, *48*, 2165.
- (22) Kreuer, K. D. *Chem. Mater.* **1996**, *8*, 610.
- (23) Goward, G. R.; Schuster, M. F. H.; Sebastiani, D.; Schnell, I.; Spiess, H. W. *J. Phys. Chem. B* **2002**, *106*, 9322.
- (24) Münch, W.; Kreuer, K. D.; Silvestri, W.; Maier, J.; Seifert, G. *Solid State Ionics* **2001**, *145*, 437.
- (25) Hickman, B. S.; Mascal, M.; Titman, J. J.; Wood, I. G. *J. Am. Chem. Soc.* **1999**, *121*, 11486.
- (26) Nakajima, H.; Sugimoto, T.; Nishikawa, O.; Nomura, S.; Honma, I. *J. Electrochem. Soc.* **2002**, *149*, A953.
- (27) Nakajima, H.; Honma, I. *Solid State Ionics* **2002**, *148*, 607.
- (28) Honma, I.; Nakajima, H.; Nishikawa, O.; Sugimoto, T.; Nomura, S. *J. Electrochem. Soc.* **2002**, *149*, A1389.
- (29) Dippel, Th.; Kreuer, K. D.; Lassègues, J. C.; Rodriguez, D. *Solid State Ionics* **1993**, *61*, 41.